OPTICAL AND DETECTOR DESIGN OF THE OCEAN COLOR INSTRUMENT FOR THE NASA PACE MISSION

U. Gliese[1], D.A. Kubalak[2], Z. Rhodes[3], C.R. Auletti[4], S.R. Babu[2], B. Blagojevic[2], K. Boggs[5], R.R. Bousquet[6], G. Bredthauer[5], G.L. Brown[2], N.T. Cao[7], T.L. Capon[2], J. Champagne[3], L.H. Chemerys[7], F.N. Chi[7], B.L. Clemons[8], J. Cook[3], W.B. Cook[2], N.P. Costen[2], K.R. Dahya[4],P.V. Dizon[2], R. Esplin[3], R.H. Estep, Jr.[2], A.R. Feizi[9], S.H. Feng[2], E.T. Gorman[8,10], J.A. Guzek[11], O.A. Haddad[12], C.F. Hakun[2], L.B. Haynes[9], M.J. Hersh[2], C.S. Hill[13], D.G. Holliday[1], L.A. Ramos-Izquierdo[2], K.S. Jepsen[7], E. Kan[2], B.P. Kercheval[7], S. Kholdebarin[9], J.J. Knuble[2], A.T. La[2], E.D. Laurila[14], M.R. Lin[2], W. Lu[15], A.J. Mariano[2], L.A. Meier[16], G. Meister[2], B. Monosmith,[8,17], D.B. Mott[8], M.M. Mulloney[1], Q.V. Nguyen[18], T.J. Nolan[7], M.A. Owens[18], J. Peterson[3], M.A. Quijada[2], K.A. Ray[7], K. Squire[3], C.P. Stull[19], J. Thomes[2], E. Waluschka[20], Y. Wen[8], M.E. Wilson[1], and P.J. Werdell[2]

1. KBR Inc, 8120 Maple Lawn Blvd., Fulton, MD 20759, USA
2. NASA Goddard Space Flight Center, Greenbelt, MD 20771, USA
3. Space Dynamics Laboratory, 416 East Innovation Ave., North Logan, UT 84341, USA
4. Aerodyne, 8910 Astronaut Blvd., Suite 208, Cape Canaveral, FL 32920, USA
5. Semiconductor Technology Associates, 1241 Puerta Del Sol, San Clemente, CA 92673, USA
6. Genesis Engineering Solutions, 4501 Boston Way, Lanham, MD 20706, USA
7. SSAI, 10210 Greenbelt Rd., Lanham, MD 20706, USA
8. Formerly of NASA Goddard Space Flight Center, Greenbelt, MD 20771, USA
9. AK Aerospace Technology, 6301 Ivy Ln., Suite 700, Greenbelt, MD 20770, USA
10. Quantum Space, 801 Thompson Ave., Rockville, MD 20852, USA
11. Design Interface, 3451 Gamber Rd., Finksburg, MD 21048, USA
12. Ingenion, 444 Seabreeze Blvd., Suite 615, Daytona Beach, FL 32118, USA
13. Aurora Engineering, 8 Cromwell Dr., Orono, ME 04473, USA
14. Peraton, 1875 Explorer St., Reston, VA 20190, USA
15. Telophase, 2111 Wilson Blvd., Suite 1150, Arlington, VA 22201, USA
16. Conceptual Analytics, 8209 Woburn Abbey Rd., Glenn Dale, MD 20769, USA
17. Newton, 5650 Rivertech Ct., Suite A, Riverdale, MD 20737, USA
18. Florez Engineering, 11718 Basswood Dr., Laurel, MD 20708, USA
19. Lentech, 7500 Greenway Center Dr., Suite 505, Greenbelt, MD 20770, USA
20. Stellar Solutions, 14425 Penrose Pl., Suite 400, Chantilly, VA 20151, USA

ABSTRACT

The Ocean Color Instrument (OCI) on NASA's Plankton, Aerosol, Cloud, ocean Ecosystem mission is a hyperspectral imager with high SNR, precision and dynamic range, and with a very low striping artifact level in the 342-887 nm wavelength range with a spectral resolution of 5 nm in 2.5 nm steps, providing a significant technological advancement over previous ocean imagers. To achieve this, OCI is designed with specialized optical imaging and opto-electronic detection systems that push the boundaries of several state-of-the-art technologies. This paper provides an overview of these systems together with their achieved performances and discussions of their key design challenges.

***Index Terms*—** Remote sensing, optical, hyperspectral, detection, focal plane

1. INTRODUCTION

The Ocean Color Instrument (OCI) [1] on NASA's Plankton, Aerosol, Cloud, ocean Ecosystem (PACE) mission is a hyperspectral imager that collects images of Earth with a 2-day global coverage, a spatial resolution of 1 km x 1 km and a spectral resolution of 5 nm in 2.5 nm steps in the 342-887 nm wavelength range. It does this with a high Signal-to-Noise Ratio (SNR) of 260-1920 in a 5 nm optical bandwidth at typical ocean spectral radiance levels and a large Dynamic Range (DR), from max-detectable signal to 1-sigma noise-floor, of 4800:1-5900:1 depending on wavelength, allowing simultaneous detection of ocean and cloud signals with no gain change, an excellent radiometric gain stability of less than ±0.1 %, and a very low spatial image striping artifact level of less than 0.1 % [2]. OCI also provides hyperspectral capability in the 322-342 nm wavelength range with reduced radiometric performance. In

addition, OCI provides 7 discrete bands in the 940-2260 nm wavelength range. In comparison, previous ocean imagers [1,3] such as SeaWiFS [4], VIIRS [5] and MODIS [6] have only provided discrete bands.

OCI employs a rotating front-end imager, two back-end slit-grating spectrographs and two Charge-Coupled Device (CCD) Time Delay Integration (TDI) cameras for the 322-887 nm wavelength range. The front-end imager creates an image of the ground scene at the input slit of the back-end spectrograph. The slit-image is re-imaged and dispersed onto the CCDs with 5 nm resolution over the entire 322-887 nm wavelength range. The rotating imager together with on-chip TDI in the CCDs are used to simultaneously achieve the critical requirements of high SNR and low image striping artifacts. It enables increased photon collection for each spatial ground scene leading to increased SNR. In addition, it creates spatial images at each wavelength using a single virtual detector thereby avoiding most spatial striping artifacts. For this to work, a high precision rotating optical system has been designed to achieve the required synchronization between the ground scene and charge movement at the CCD surface.

With its hyperspectral capability and high performance, OCI provides a significant technological advancement enabling quantitative evaluation of separate plankton species from space for the first time. This high-performance hyperspectral capability is expected to also find other beneficial scientific uses. To achieve the performance, OCI is designed with specialized optical imaging and opto-electronic detection systems that push the boundaries of several state-of-the-art optical and opto-electronic technologies. The performance and unique design challenges of the optical imaging and opto-electronic detection systems are presented in this paper.

2. OPTICAL IMAGING SYSTEM

The OCI optical imaging system is shown in Fig. 1. The 322-2260 nm front-end optical imager is a rotating mirror-based system that images the ground scene onto a slit with an Instantaneous Field Of View (IFOV) of 16 km x 1 km. The scan-rate is 5.77 Hz and the IFOV is scanned over an angular range of ±56.6° for a ground swath-width of 2663 km. Further, it includes a depolarizer to ensure a low polarization sensitivity of less than 1 %. The image rays are reflected of a Half Angle Mirror (HAM), spinning at 2.885 Hz, onto the slit to ensure the scanned IFOV is always aligned to the slit. The back-end optical spectrograph consists of two slit-grating spectrographs for the 322-607 nm and 597-887 nm wavelength ranges, and a fiber-coupled filter-bank spectrograph for the 940-2260 nm wavelength range. The three ranges are separated using dichroic beam-splitters in collimated space.

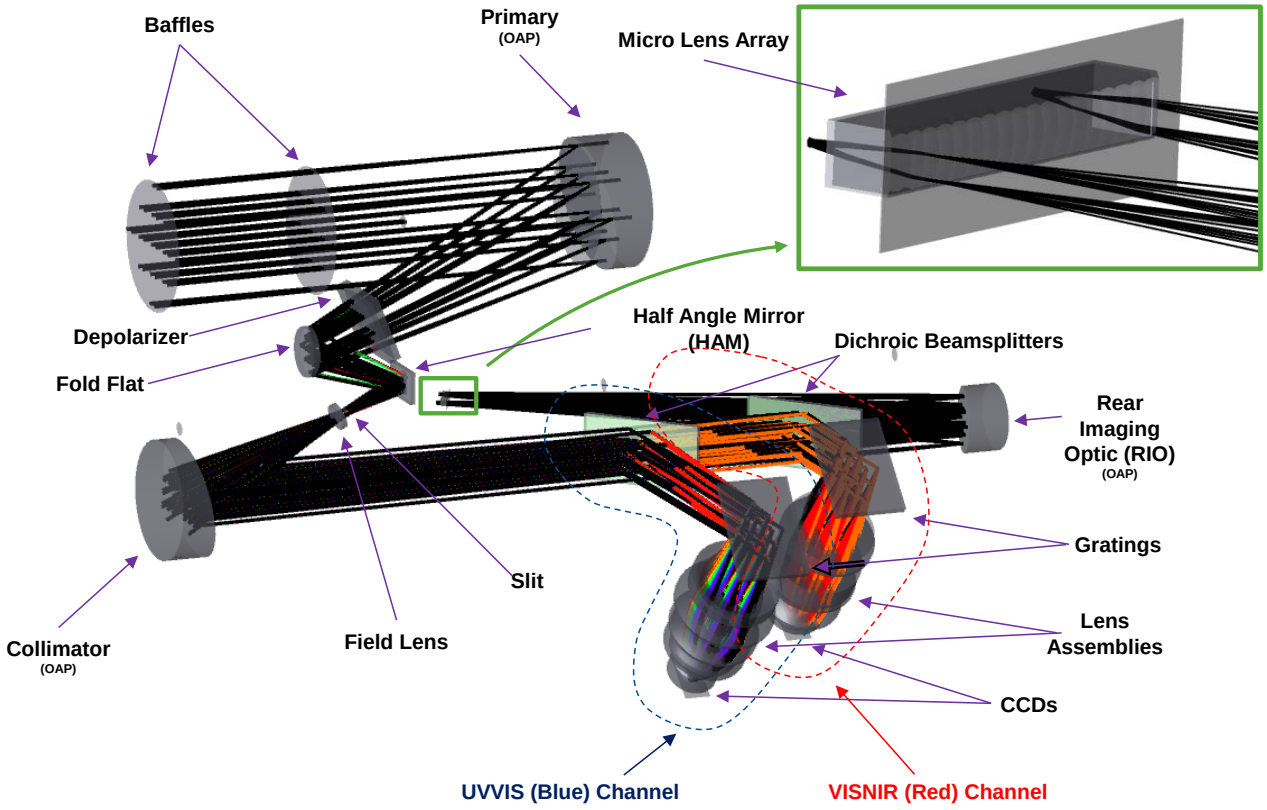

Fig. 1: Optical imaging system.

For the two hyperspectral ranges, the slit-image is dispersed by two gratings and re-imaged onto two 128x512 CCDs using two complex lens-assemblies. Each dispersed slit-image maps to 128x8 pixels of 26 µm x 26 µm on the CCDs. For the 940-2260 nm range, the slit-image is re-imaged onto a 16x1 Micro-Lens Array (MLA) that effectively acts as the focal plane since each lens element is fiber coupled to wavelength filtered Photo Diodes (PDs).

Optical system performance:

- Throughput: ≥ 0.4 at ≥ 360 nm (0.3 at 340 nm)
- f-number: 1.2
- Polarization sensitivity: ≤ 1 % (≤ 0.2 % at ≥ 360 nm)
- Point Spread Function (PSF): ≤ 46 µm (80 % energy)
- Modulation Transfer Function (MTF): ≥ 0.95 (Nyquist)
- Spectral sampling: 0.625 nm
- Out-Of-Band Response Ratio (OOBRR) ≤ 0.05 (integrated out-of-band to in-band ratio for 5 nm resolution full-width 1 %)

These achieved performances are demanding for the design and involved optical technologies. The front-end optical system has to work over the entire 322-2260 nm wavelength range with high throughput to achieve high SNR. For this, the back-end hyperspectral spectrographs also require a challenging very low f-number. Maximizing throughput of a system with such a broad wavelength range and with so many surfaces is difficult. Unique coatings for both the reflective and transmissive optics had to be created to extend performance into the UltraViolet (UV). Careful choice of lens materials also had to be made in order to maximize throughput. The f-number, together with the broad spectral range, UV requirements, IFOV and widely dispersed image rays, leads to a very difficult back-end design. Despite this, a narrow Point Spread Function (PSF) has been achieved which is essential for the high MTF and low OOBRR. The number of elements, material choices, and element radii all had to be carefully balanced to meet requirements without causing other problems, such as ghosting due to steep lens curvatures.

For the OCI architecture to work, it is essential that the spinning of the primary mirror sub-system and the HAM are closely synchronized. At the same time the movement of the ground scene through the slit and therefore across the CCDs must be precisely synchronized with the TDI charge movement in the CCD. This is ensured using state-of-the-art motors together with precision phase-locked loop motor control locked to track the CCD charge movement clock.

3. UVNIR DETECTION SYSTEM

The hyperspectral UV to Near InfraRed (UVNIR) opto-electronic detection system, as shown in Fig. 2, consists of an UV to VISible (UVVIS) Focal Plane Assembly (FPA) and a VIS to Near InfraRed (VISNIR) FPA, each containing

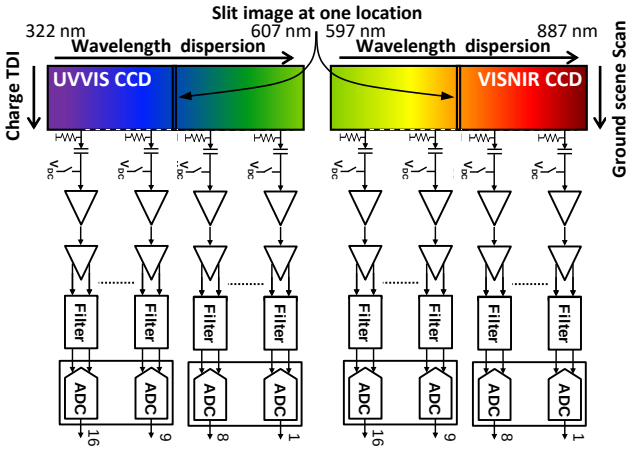

Fig. 2: Hyperspectral UVNIR detection system.

a 128x512 pixel Si CCD with 16 readout channels of 32 columns per channel operated in on-chip TDI mode and a Front-End Electronics (FEE) board with DC-clamps, amplifiers, noise filters and fast, low-power 8-channel 14-bit Analog-to-Digital Converters (ADCs). A Data Acquisition Unit (DAU) provides bias and clocking to the FPAs, acquires digital data from the FPAs and performs data processing in form of Correlated Double Sampling (CDS) and digital aggregation of 8x8 pixels into one Science Pixel (SP) corresponding to 1 km x 1 km on the ground. The DAU also synchronizes with the motor controller to ensure the ground scene scan is locked to the TDI charge movement.

UVNIR detection system performance:

- QE: ≥ 0.4 (315 nm), ≥ 0.97 (460 nm), ≥ 0.91 (605 nm)
  ≥ 0.94 (600 nm), ≥ 0.97 (680 nm), ≥ 0.67 (890 nm)
- Full well capacity: ≥ 750 ke-
- Read speed: 8.5 MHz with 17 MHz CDS
- Gain: 22, 33 and 55 DN_{14}/ke- (depending on channel)
- Noise: ≤ 3 DN_{14} 1-sigma
- Precision: ≤ 0.1 %
- Channel-Channel (Ch-Ch) Crosstalk: ≤ $1.3 \cdot 10^{-4}$
- DR: 4800:1-5900:1 (max-detectable signal to 1-sigma noise)
- Step recovery precision (max → min): 0.25 % within 1 SP

To achieve the required OCI spatial and spectral resolution, the CCDs have to be operated at a high read-speed leading to low precision. A high MTF and low OOBRR require high Charge Transfer Efficiency (CTE) and low Ch-Ch crosstalk in the CCDs. They are implemented with high CTE as well as high output channel density to reduce read speed as much as possible in trade-off with crosstalk. Another main challenge is to simultaneously achieve high DR, low noise (for high SNR) and high precision. Low noise requires narrow bandwidth and high precision requires fast settling time (wide bandwidth) or low read speed. The high DR requires large CCD well and sense node capacity together with a 14-bit ADC further challenging settling time. The

CCD and electronics have been carefully designed to accomplish the best possible trade-off between these opposing demands. Finally, as full settling of the CCD output signal cannot be attained while achieving the required DR and noise, it is critical that the CCD clock jitter and bias are very stable to reach the required high read precision.

4. SWIR DETECTION SYSTEM

The 7-band 940-2260 nm ShortWave InfraRed (SWIR) opto-electronic detection system consists of a focal plane in the form of a 16x1 MLA where each lens corresponds to a 1 km x1 km SP on the ground. The MLA is fiber coupled to 16 SWIR Detection Sub-assemblies (SDSs). Each SDS contains optics splitting the input out to two band filters that are each followed by a PD and a FEE feeding analog signals into a multi-channel 16-bit ADC. Varying amounts of the 32 PDs are assigned to each of the 7 bands and digital TDI is applied after detection. Both InGaAs and HgCdTe PDs are used depending on wavelength.

SWIR detection system performance:

- QE: ≥ 0.8
- Gain: $5.24 \cdot 10^5 - 5.38 \cdot 10^5$ $DN_{16}/\mu W$ (depending on channel)
- Noise: ≤ 6.3 DN_{16} 1-sigma
- Precision: ≤ 0.2 %
- DR: 9600:1-20000:1 (max-detectable signal to 1-sigma noise)
- Pulse response (max → min): 1 % within 3 SP

Achieving low leakage between the lens elements in the MLA is important for high MTF presented a significant challenge that required development of special fabrication techniques. Electronically, this is a very different system than the UVNIR system. This system uses direct photo detection of each SP so the sampling speed is low at 23.2 kHz. However, the cloud level signals and very low-level ocean signals demand a high DR and low noise. This requires a large area PD (290 µm diameter), very high gain, 16-bit ADC and a narrow bandwidth. In contrast, high MTF and precision require a wide bandwidth and a fast pulse response. Careful design had to be done to achieve a stable circuit capable of the high gain with a wide enough bandwidth. Further, detailed modeling was done to optimize the bandwidth for best possible trade between noise and MTF. A fast pulse response was not achieved due to a long-tail pulse response of the PDs and limitations of the FEE design [7]. Development of an in-flight pulse response measurement system and a post-processing method ensures high precision.

5. CONCLUSION

Outstanding performance is achieved for OCI despite the constraints posed by state-of-the-art technologies. A wide range of technology developments and design optimizations were carried out for this. With its advanced optical imaging and detection system, OCI is set to deliver a significant advancement in the ocean, cloud and aerosol sciences.

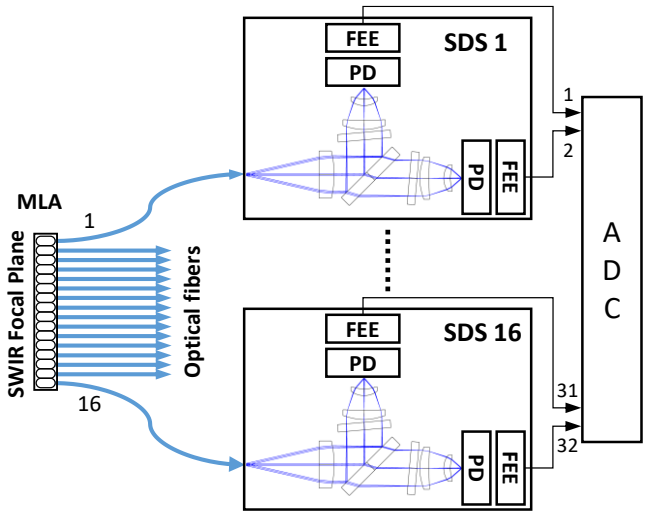

Fig. 3: 7-band SWIR detection system.

6. ACKNOWLEDGEMENTS

The authors would like to thank the following companies for their contributions to the design and involved technologies: Acktar, Advanced NanoPhotonics, Alluxa, Bach, BEI, Corning, Ingeneric, Leonardo, Markury Scientific, NuTek, Onyx, Optimax, RMI, Ruda Optical, Semiconductor Technology Associates, Teledyne Judson Technologies, Thin Gap, TNO, Viavi, Zecoat.

7. REFERENCES

[1] P.J. Werdell, et. al., "The Plankton, Aerosol, Cloud, Ocean Ecosystem Mission: Status, Science, Advances," Bulletin of the American Meteorological Society, Vol. 100, Issue 9, pp. 1775-1794, 2019

[2] G. Meister, et al., "Initial Look at the Results from the Prelaunch Characterization Campaign of OCI on the PACE Mission", TH1.R6: NASA PACE Mission, IGARSS 2023

[3] C.R. McClain, et. al., "Genesis and Evolution of NASA's Satellite Ocean Color Program," Frontiers in Remote Sensing, Vol. 3, Article 938006, pp. 1-19, 2022.

[4] C.R. McClain, et. al.,, "An overview of the SeaWiFS project and strategies for producing a climate research quality global ocean bio-optical time series," Elsevier Deep-Sea Research II, Vol. 51, Issues 1-3, pp. 5-42, 2004.

[5] R.E. Murphy, et. al., "The Visible Infrared Imaging Radiometer Suite," Earth Science Satellite Remote Sensing, Springer, Berlin, Heidelberg, ISBN 978-3-540-35606-6, pp. 199-223, 2006

[6] W.E. Esaias, et. al., "An Overview of MODIS Capabilities for Ocean Science Observations," IEEE Transactions on Geoscience and Remote Sensing, Vol. 36, No. 4, pp. 1250-1265, 1998.

[7] U. Gliese, et. al., "Pulse response of the short-wave infrared detection system of the ocean color instrument for the NASA PACE mission," Submitted for SPIE Sensors + Imaging 2023.